Design and Demonstration of an Infrared Meanderline Phase Retarder

Jeffrey S. Tharp, Brian A. Lail, *Senior Member, IEEE*, Ben A. Munk, *Life Fellow, IEEE*, and Glenn D. Boreman, *Senior Member, IEEE*

***Abstract*—We compare design and measurements for a single-layer meanderline quarter-wave phase retarder, operating across the wavelength range from 8 to 12 micrometers (25 to 37.5 THz) in the infrared. The structure was fabricated using direct-write electron-beam lithography. With measured frequency-dependent material properties incorporated into a periodic-moment-method model, reasonable agreement is obtained for the spectral dependence of axial ratio and phase delay. As expected from theory, the single-layer meanderline design has relatively low throughput (23%), but with extension to multiple-layer designs, the meanderline approach offers significant potential benefits as compared to conventional birefringent crystalline waveplates in terms of spectral bandwidth, angular bandwidth, and cost. Simple changes in the lithographic geometry will allow designs to be developed for specific phase retardations over specified frequency ranges in the infrared, terahertz, or millimeter-wave bands, where custom-designed waveplates are not commercially available.**

***Index Terms*—Frequency selective surfaces, infrared measurements, polarization.**

I. Introduction

MEANDERLINE wave plates [1]–[5] have been traditionally used in the radio frequency (RF) portion of the spectrum to convert linearly polarized radiation into circularly polarized radiation. The meanderline structure acts as a phase retarder for the two orthogonal wave components that are polarized along and perpendicular to the meander axis. The meanderline acts primarily as an inductive element along the meander axis and as a capacitive element perpendicular to the meander axis, creating the relative phase delay for the orthogonal polarization components. Use of electron-beam lithography has made fabrication of such structures feasible at much higher frequencies, up into the infrared (IR) portion of the spectrum. The ease of fabrication, low fabrication costs, and compact construction may provide a potentially important alternative to birefringent crystals in the IR, THz, and millimeter-wave bands. An especially attractive characteristic of meanderline waveplates is the ability to define designs for specific frequencies and phase delays by simple changes in the lithography. This flexibility offers the primary benefit as compared to birefringent crystals. This is because the wavelength of operation for a birefringent crystal quarter-wave plate is determined by the thickness of a given material and its optical properties. The current wavelengths common for commercial retarders is from visible to $\sim$2.1 μm, though they can be found at 10.6 μm, i.e., Zn(SO_4). In the range of interest (8–12 μm) there are very few alternatives as it is difficult to find materials in this range that have both birefringence and transparency for the entire band. In the THz, there are essentially no alternatives as of yet since material characterization in the THz spectral region is in relative infancy as compared to the long-wave IR (LWIR) and visible. Therefore, meanderlines are a potential substitute as they are broadband and the center wavelength can be tuned by changing the geometry. Advantages are expected in the areas of spectral and angular bandwidth as well, compared to traditional birefringent crystal waveplates. The bandwidth of the best single-order quarter-wave plate theoretically is fairly broad and is limited to the $1/\lambda$ dependence of the optical path difference. The typical range is $\pm 15\%$ of the central wavelength with an axial ratio (AR), the ratio of the electric field magnitude along the major axis to the minor axis of the polarization ellipse, less than 1.5 for a true single-order quarter-wave plate. The more common and cheaper multi-order quarter-wave plates have much narrower bandwidths performing with an axial ratio less than 1.5 for a range of $\pm 0.5\%$ of the central wavelength. The multi-order retarders are so narrow banded because the change in phase delay with respect to the wavelength is proportional to the phase delay itself. The typical multi-order quarter-wave plate in the visible is $\sim$0.7 mm thick quartz which corresponds to a retardation of 11.25 waves. A single-order quarter-wave plate has a retardance of 0.25 waves and is therefore almost 50 times less sensitive to dispersion.

In this paper, we present a design for a broadband quarter-wave plate (QWP), which operates over the 8 to 12-micrometer wavelength band in the IR. We analyze the structure with a method-of-moments technique, using measured frequency-dependent material characteristics for the dielectric and metallic layers. Relatively good agreement is obtained between modeling and measurements for the spectral dependence of axial ratio and relative phase delay for the fabricated meanderline, with better modeling accuracy at the long-wavelength end of the measured band. Finally, we discuss ways to improve the power throughput of such structures.

The present proof-of-concept demonstration is significant because it shows that meanderline structures can be fabricated for IR operation using available lithographic techniques. Furthermore, although the high-frequency properties of metals are not as ideal as in the RF band, potentially useful devices can be developed with viable performance levels.

Manuscript received August 1, 2006; revised April 6, 2007.

J. S. Tharp and G. D. Boreman are with the CREOL College of Optics and Photonics, University of Central Florida, Orlando, FL 32816 USA.

B. A. Lail is with the Department of Electrical and Computer Engineering, Florida Institute of Technology, Melbourne, FL 32901 USA.

B. A. Munk is with the ElectroScience Laboratory, Ohio State University, Columbus, OH 43210 USA.

my hopes were

Digital Object Identifier 10.1109/TAP.2007.908369

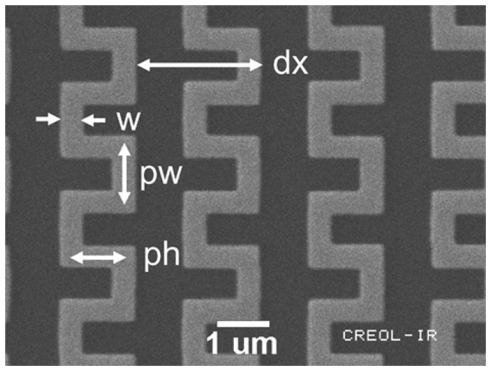

Fig. 1. Electron micrograph of a fabricated Au meanderline structure on a high-resistivity Si substrate showing the definition of the geometrical variables.

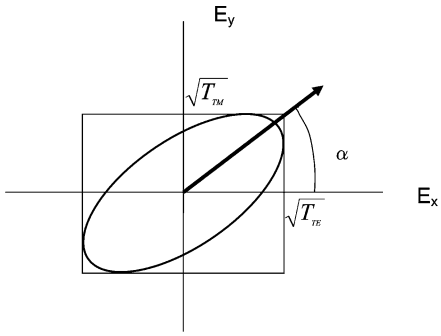

Fig. 2. Diagram of the auxiliary angle with respect to the polarization ellipse.

II. Modeling

The meanderline phase retarder was designed using of Ohio State's Periodic Method of Moments (PMM) software package. The method solved for the excited currents by representing the meander structure as a series of connected dipoles and applying periodic boundary conditions. The periodic boundary conditions allowed for an infinite array of structures to be represented as a unit cell of finite geometry. The geometrical variables, as shown in Fig. 1, were: pulse width (pw), pulse height (ph), width (w), and periodicity (dx). When defining the unit cell for PMM, we extended one arm of the meanderline outside of the periodic boundary to simulate continuity.

Frequency-dependent material parameters were measured in the IR band of interest using a commercial infrared variable-angle spectroscopic ellipsometer (IR-VASE), capable of measurements over a 1-μm to 30-μm range. The substrate material was characterized using a complex permittivity function, and the metallic meanders were modeled using a sheet-resistance function developed using measured frequency-dependent conductivity and material thickness. These material characteristics were read in to PMM with an external MATLAB interface code [6].

The meanderline has an equivalent complex wave impedance that the incident field experiences for each polarization, both along and perpendicular to the meander axis. The mismatch between the meanderline layer impedance and that of the surrounding dielectric causes reflections that affect both the magnitude and phase of the transmitted and reflected fields. The difference in phase that is induced in the transmitted fields gives the retarder its function. With perfectly conducting meanderlines, this impedance is completely imaginary since there is no loss in the resonant currents. This implies that an ideal meanderline will only increase the impedance mismatch at a two dielectric interface while not changing the real part of the impedance mismatch between the meanderline/dielectric combination, thereby increasing the reflection. However, in the IR metals tend to be more resistive and thus will contribute a minor real part to the impedance.

With this frequency-dependent PMM model, we were able to compute the power transmission coefficients along and perpendicular to the meander axis, $\mathrm{T_{TE}}$ and $\mathrm{T_{TM}}$, along with the phases of the respective transmitted fields, δ_{TE} and δ_{TM}. From these outputs we can compute the polarimetric parameters of interest. A meanderline acts as a phase retarder for radiation linearly polarized at an angle of 45° to the meander axis. To simplify the computation of AR using direct output variables from PMM, we used the angle along the diagonal of a rectangle circumscribing the polarization ellipse as the auxiliary angle (α shown in Fig. 2) and the relative phase delay (δ) between the orthogonal transmitted field components

$$\alpha = \tan^{-1}\sqrt{\frac{\mathrm{T_{TE}}}{\mathrm{T_{TM}}}} \quad \text{and} \quad \delta = \delta_{\mathrm{TE}} - \delta_{\mathrm{TM}}. \tag{1}$$

The AR is then given as [7]

$$\mathrm{AR} = \tan[1/2\sin^{-1}(\sin 2\alpha \sin\delta)]^{-1}. \tag{2}$$

In these variables, for example, circular polarized radiation would have an $\mathrm{AR} = 1, \alpha = 45°$, and $\delta = \pm 90°$.

The performance of a meanderline is governed both by the geometric variables and the material parameters. The overall size scale of the geometric variables is determined through the effective permittivity of the substrate (value intermediate between that of the substrate and of air). The dimensions of the structure variations should be smaller than the free-space wavelength divided by the square root of the effective permittivity to avoid generation of grating lobes from the periodic structure. In addition, the closer the structures are to one another, i.e., smaller *dx* or larger w, the larger the impedance mismatch that contributes to a larger phase delay.

Another variable that governs the performance of the meanderline structure is the angle of incidence of impinging radiation. This would be of particular interest if the meanderline retarder is placed in an optical system. The angle-of-incidence performance was modeled for the meanderline structure that was to operate as a quarter-wave retarder. The model was run for the incident angles of 0°, 5°, 10°, and 15° with the plane of incidence both along and perpendicular to the meanderline axis. The resulting modeled AR and phase delay is shown in Fig. 3. The modeled data shows the AR minimum shifting to lower wavelengths and the phase delay decreasing as the incident angle is increased. Future work will involve measuring the fabricated structure at these angles.

The design goal for the meanderline that functions as a quarter-wave plate was to have an axial ratio that remained less than 1.5 over the 8μm to 12 μm band at normal incidence.

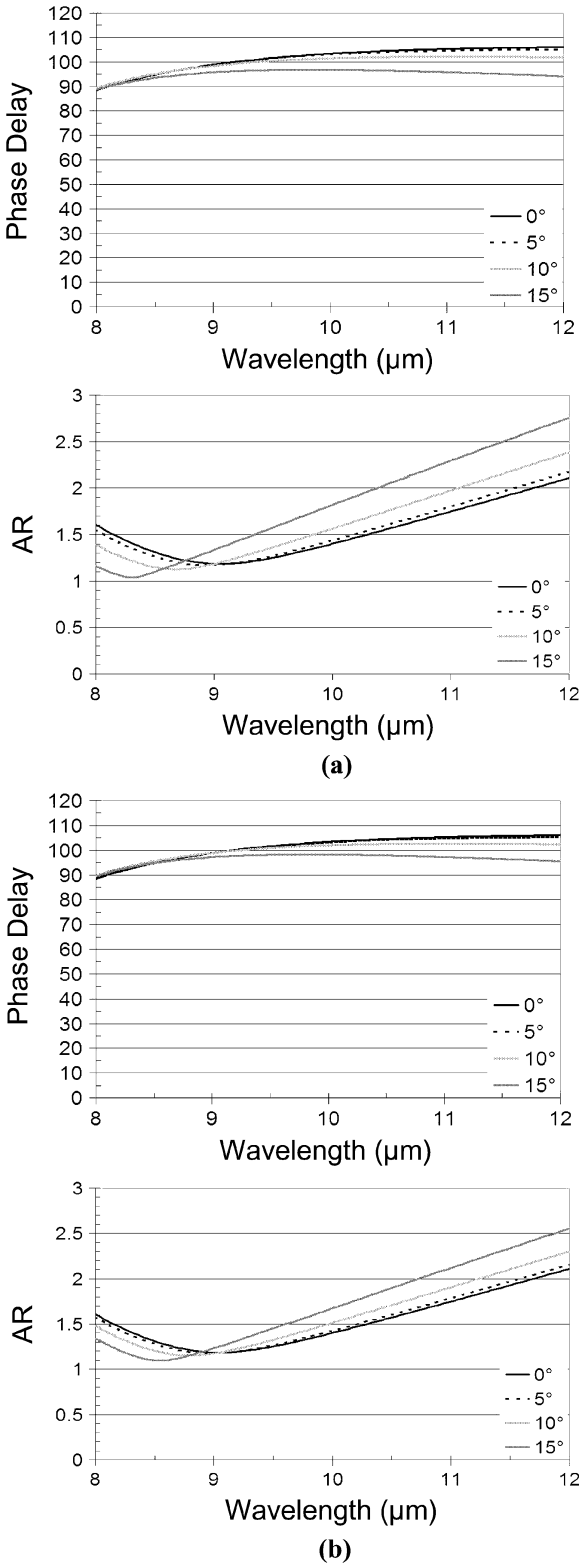

Fig. 3. Plots of the modeled phase delay and axial ratio for the quarter-wave plate meanderline design for incident angles of 0°, 5°, 10°, and 15° for radiation incident from (a) along the meanderline axis and (b) perpendicular to the meanderline axis

This goal was to demonstrate the broad bandwidth potential as compared to the best performance for a birefringent crystal operating at 10.6 μm.

III. Fabrication and Measurements

The minimum dimensions of the desired meander structures were less than half a micrometer, so electron-beam lithography processes were used for fabrication. The resolution limit of the Leica 5000+ electron-beam writer was on the order of 25-nm line widths allowing for a high-fidelity reproduction of our design geometry. The substrate for the structure was chosen to be a high-resistivity (3–5 k Ω cm) Si wafer, because of the necessity for a high degree of electrical insulation between closely-adjacent structures. In addition, high-resistivity Si exhibits minimal material attenuation over the 8–12 μm band of interest. However, high reflection losses are expected since Si has a relative permittivity of 11.5 over this band. The final fabricated structures had an overall dimension of 1cm^2.

Performance characterization of the meanderline structures used the IR-VASE to measure $\tan(\alpha)$ and δ over the 8–12 μm wavelength range of interest. From the $\tan(\alpha)$ and δ data, AR values were computed as a function of wavelength using (2). In addition, the percentage of the transmitted radiation in the desired polarization state, the degree of polarization, was also measured using the IR-VASE.

IV. Results and Discussion

Our overall design goal was to develop a meanderline quarter-wave plate (QWP), which would operate over the 8–12 μm wavelength band. To begin the development process, we first designed an IR meanderline structure simply to change the transmitted polarization with respect to its initial state as a proof-of-concept. The design geometry for the first structure (shown in Fig. 1) was: pw $= 1.0$ μm, ph $= 1.0$ μm, $w = 0.4$ μm, and $dx = 2.3$ μm. This design was modeled, fabricated, and then characterized using the IR-VASE. A comparison between the modeled and measured spectral dependence of δ and AR is shown in Fig. 4(a) and (b), along with the modeled spectral dependence of $\mathrm{T_{TE}}$ and $\mathrm{T_{TM}}$ in Fig. 4 (c). The large short-wavelength AR showed that the transmitted radiation was nearly linearly polarized. This was consistent with the large short-wavelength difference between $\mathrm{T_{TE}}$ and $\mathrm{T_{TM}}$. For longer wavelengths, these transmissions become closer, reducing the AR. Within the band of interest, an AR of 1 was not achieved in this design. At longer wavelengths, the measured and modeled values for AR agreed quite well, and the transmitted radiation approached an elliptical polarization state with an AR less than 2 from 10 to 12 μm. The modeled and measured spectral values of δ agreed within 15° from 9 to 11 μm, with significant divergence only at the short-wavelength end of the band. It is of interest to note that the measured phase delay was quite broadband, showing a near-constant value around 60° from 9 to 12 μm. The modeled power throughput of the design was 41% at 10.6 μm, which compared well to the CO_2-laser measured throughput of 38% at 10.6 μm, and the degree of polarization was measured to be 88%.

The reasonable agreement between PMM modeling and measurements for this initial design encouraged us to attempt a design for a broadband QWP over the 8–12 μm band. To function as a QWP, we needed to increase δ to 90° and to make $\mathrm{T_{TE}}$ and $\mathrm{T_{TM}}$ equal, yielding an $\mathrm{AR} = 1$. Due to the inherent spectral dispersion of the structure, our design goal was to have an AR

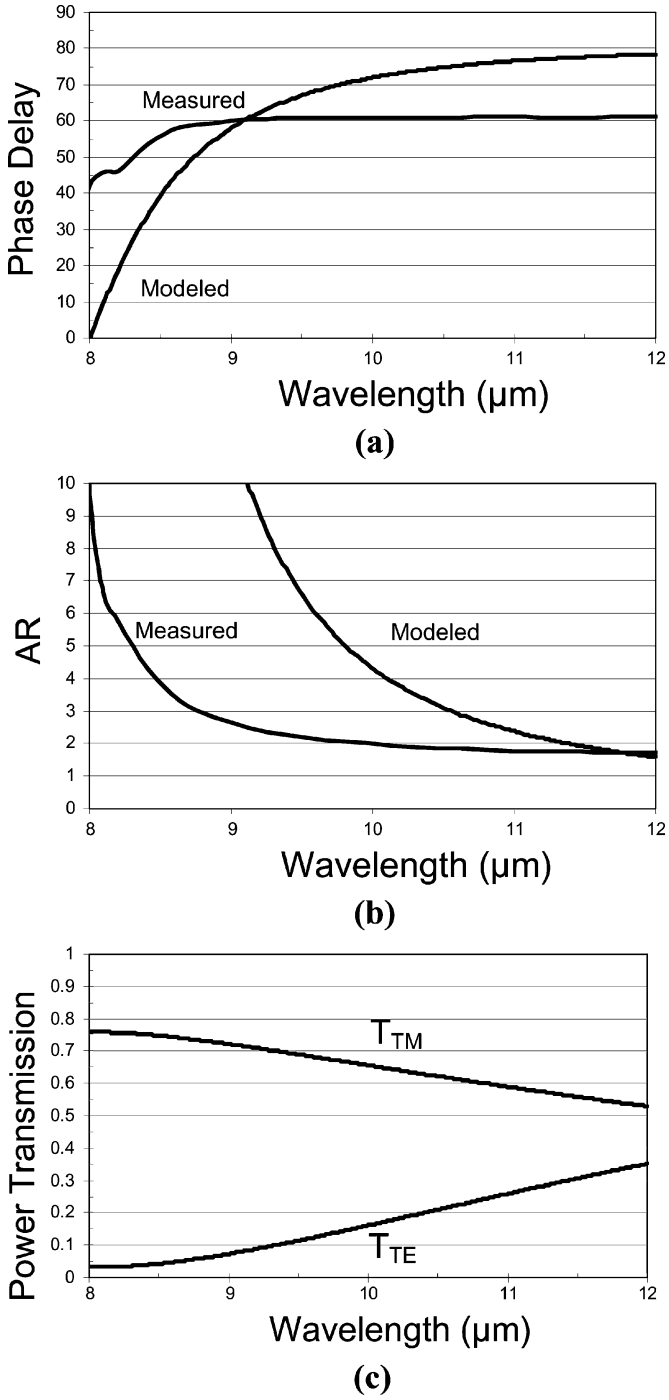

Fig. 4. Plots of modeled and measured spectral quantities for the proof-of-concept meanderline design for: (a) relative phase delay, (b) axial ratio, and (c) plot of modeled orthogonal power transmission coefficients.

as close to 1 as possible at a near central wavelength of 9.2 μm while having the spectral AR remain less than 2 over 8–12 μm. This structure would have a retarding performance approaching that of a true single-order crystal waveplate. The materials that were used were the same as in the first design, so the only differences in the design were the geometric parameters. To increase δ, we increased the line widths and decreased the periodicity and in that fashion we varied the design until our goals were met in the PMM-computed results. Our optimization proceeded toward the design goals under the constraint that each of the parameters

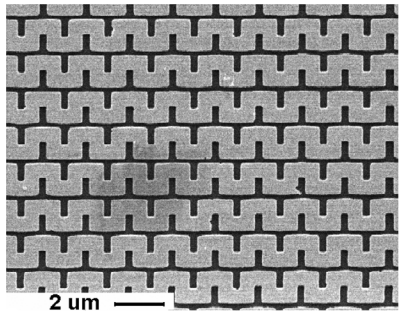

Fig. 5. Electron micrograph image of the fabricated quarter-wave plate design.

had to be a multiple of 0.05 μm to remain within the fabrication tolerances. The optimized single-layer QWP design, shown in Fig. 5, used $\mathrm{pw} = 0.9$ μm, $\mathrm{ph} = 0.7$ μm, $w = 0.6$ μm, and $dx = 1.6$ μm. The comparison between the computed and measured spectral values of δ and AR for this structure, along with computed spectral dependence of $\mathrm{T_{TE}}$ and $\mathrm{T_{TM}}$, are shown in Fig. 6. The uncertainty in the measurement of δ is $\pm 0.5^\circ$ and α is $\pm 0.25^\circ$ and remained constant over the 8–12 μm band. This leads to a measurement error in the AR of ± 0.01at the δ and α values corresponding to an AR ~ 1 with the maximum error occurring near 8 and 12 μm with the AR error of ± 0.03.

Once again, the PMM models agree fairly well to the measured values for AR and the relative phase delays, and the design goals for a broadband QWP were nearly met over most of the band. The measurements show an AR ≤ 2 over the entire 8–12 μm spectral range and a relative phase delay of $90^\circ \pm 9^\circ$ from 9.5–12 μm. The PMM-computed power throughput was 24% at 10.6 μm, while the CO_2 -laser-measured throughput at this wavelength was 23%. The correlation between the modeled and measured values of δ is similar to the proof-of-concept design in that the agreement is better in the longer wavelengths. The AR shows good agreement, except that the wavelength for $\mathrm{AR} \approx 1$ is at about 10.5 μm rather than the design wavelength of 9.2 μm. The design wavelength for $\mathrm{AR} = 1$ is determined by the wavelength where $\mathrm{T_{TE}}$ and $\mathrm{T_{TM}}$ are equal in magnitude since, as seen in Fig. 6(a), the relative phase delay was expected to be fairly constant and near 90°. The deviation in the measured $\mathrm{AR} = 1$ design wavelength from the modeled one could be caused by the rapid variation with wavelength for $\mathrm{T_{TE}}$ and $\mathrm{T_{TM}}$. The orthogonal transmission coefficients vary greatly over the entire band, shown in Fig. 6(c), and the gradient of the spectral variation is very sensitive to the impedance of the meanderline structure.

The throughput of the single-layer meanderline QWP was 23%, which was low compared to commercially available QWPs that typically have a throughput of around 98% at the design wavelength. We are presently involved in research aimed at improving the transmittance of IR meanderline structures.

The transmitted power budget as measured included an expected 45% dielectric reflection loss from the two surfaces of the Si substrate as measured using a Fourier transform IR spectrometer (FTIR). The Si wafer used was 380 μm in thickness. In the Fourier transform setup used in the measurement, the Fabry–Perot resonances are so close together that no interference effects were observed. The meanderline retarder primarily

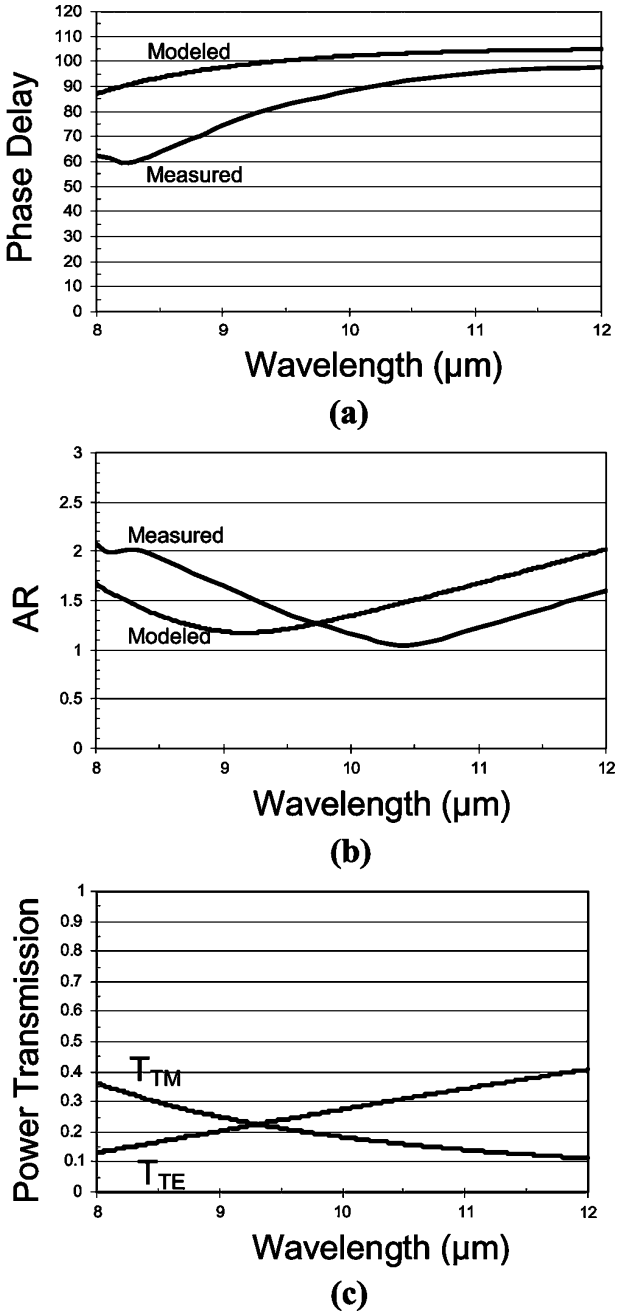

Fig. 6. Plots of modeled and measured spectral quantities for the quarter-wave plate meanderline design for (a) relative phase delay, (b) axial ratio, and (c) plot of modeled orthogonal power transmission coefficients.

has an imaginary impedance and therefore it will only increase the impedance mismatch at the silicon/air interface. Therefore the mismatch in wave impedance due to the interaction at the Si/meanderline/air boundary causes a large reflection loss. There are also minor losses that are going to be due to the resistive nature of the gold at these frequencies.

The reflection losses can be reduced by use of lower permittivity substrates, or perhaps by implementation of antireflection coatings on the substrate. However, any such coating on a surface that is in contact with the meanderlines will influence the effective permittivity and therefore change the geometry of the meanderline for a particular design performance. Reflection losses may be lowered somewhat by optimization of the metal thickness, which has the potential to change the impedance of the meanderlines via the sheet resistance. These losses can also be reduced by the use of multiple meanderline layers to improve impedance matching by reducing the mismatch at each layer [5].

If it indeed proves possible to increase the throughput, the meanderline-retarder approach stands to have some significant advantages compared to crystalline waveplates. There are no commericially available crystal waveplates for the THz and mmW bands, so a meanderline retarder would be an enabling technology in these bands. The meanderline can be easily designed and fabricated to operate at any arbitrary wavelength of interest by varying the geometry and surrounding dielectric materials. The material requirements for the meanderline are also more forgiving than for crystal waveplates since the only requirement is that the substrate is transparent, rather than transparent and birefringent, to the incident radiation. The meanderline also has advantages of weight and compactness, reduced optical path, and simplicity of fabrication within the performance limits of lithography.

V. Conclusion

Two IR meander designs fabricated and tested, with reasonably good agreement between results of the frequency-dependent PMM model and measurements of AR, δ and throughput. The performance of the quarter-wave plate design ($\mathrm{AR} \leqslant 2$ over 8 to 12 μm and $\delta = 90^\circ \pm 10\%$ over 9.5 to 12 μm) verifies the possibility of broadband retarders in the IR. The current quarter-wave plate design shows low throughput (23%) as compared to other technologies, however the loss mechanisms have been identified and research is ongoing to increase the throughput. The ongoing research includes the investigation of lower permittivity substrate materials and the implementation of multiple-layer meanderlines for reduction of re-radiation loss. Work will also commence on characterizing the meanderline for non-normal angles of incidence to determine the correlation to the modeled expectations as the change is expected to be fairly minor.

The meanderline is a potentially significant technology for IR, THz and mmW bands where commercial waveplates are not available. The feasibility of custom tailored phase retarders will offer an ability to extend polarimetric analysis and material characterizations to these new bands of interest.

References

[1] L. Young, L. Robinson, and C. Hacking, "Meander-line polarizer," *IEEE Trans. Antennas Propag.*, vol. 21, no. 3, pp. 376–378, May 1973.

[2] M. Mazur and W. Zieniutycz, "Multi-layer meander-line polarizer for Ku band," *Microw., Radar, Wireless Commun.*, vol. 1, pp. 78–81, 2000.

[3] J. Zürcher, "A meander-line polarizer covering the full E-band (60–90 GHz)," *Microw. Opt. Technol. Lett.*, vol. 18, no. 5, pp. 320–323, Aug. 1998.

[4] T. K. Wu, "Meanderline polarizer for arbitrary rotation of linear polarization," *IEEE Microw. Guided Wave Lett.*, vol. 4, pp. 199–201, Jun. 1994.

[5] B. A. Munk, *Finite Antenna Arrays and FSS (Appendix C)*. New York: Wiley-IEEE Press, Jul. 2003, ISBN 0-471-27305-8.

[6] J. Ginn, B. Lail, D. Shelton, J. Tharp, W. Folks, and G. Boreman, "Modeling infrared frequency selective surfaces with frequency dependent materials," in *Proc. 22nd Int. Review of Progress in Applied Computational Electromagnetics (ACES 2006)*, Miami, FL, Mar. 12–16, 2006, pp. 307–311.

[7] D. Goldstein, *Polarized Light 2ed.*. New York: Marcel Dekker AG, 2003, ISBN 0-8247-4053-X.

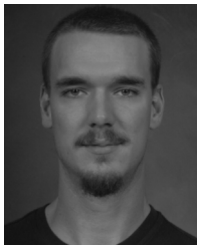

Jeffrey S. Tharp received the B.S. degree in physics from the University of North Carolina at Asheville and the M.S. degree in optical science and engineering from the University of North Carolina at Charlotte, in 2002 and 2004, respectively. He is currently working toward the Ph.D. degree in optics at the University of Central Florida, Orlando.

He is with the College of Optics and Photonics (CREOL) where he is a member of the Infrared Systems Research group. His current research interests include polarization modification using infrared frequency selective surfaces.

Brian A. Lail (S'94–M'02–SM'07) received the B.S. degree in physics from Furman University, Greenville, SC, and the M.S. degree in physics from New Mexico State University, Las Cruces, in 1991 and 1994, respectively, and the M.S and Ph.D. degrees in electrical engineering from New Mexico State University, Las Cruces, in 1998 and 2002, respectively.

From 2002 to 2005, he was with the Department of Electrical and Computer Engineering at the University of Central Florida, Orlando. Since 2005, he has been an Assistant Professor in the Department of Electrical and Computer Engineering at Florida Institute of Technology, Melbourne, teaching and conducting research in applied and computational electromagnetics.

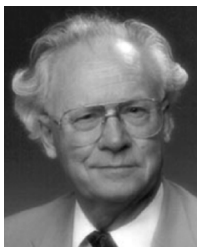

Ben A. Munk (M'61–SM'85–F'89–LF'96) received the M.S. degree in electrical engineering from the Technical University (Polytechnical Institute) of Denmark and the Ph.D. degree in electrical engineering from The Ohio State University (OSU), Columbus, in 1954 and 1968, respectively.

He joined the ElectroScience Laboratory (ESL), OSU, in 1964 where he is currently a Professor of electrical engineering and a Supervisor. Prior to joining ESL, he was a Chief Designer for A/S Nordisk Antenne Fabrik, Denmark, and an Assistant Group Leader in the antenna section of Rohde and Schwarz in Munich, Germany. Later, he was a Research and Development Engineer with the Andrew Corporation, Chicago, IL, and then an Antenna Research Engineer with the Rockwell Corporation, Columbus, OH. He has been a Consultant to several of the major airplane and satellite companies in the U.S. and he sits on a number of government committees. He has been the advisor for more than 75 Ph.D. and M.Sc. students, many of whom have become successful leaders in industry and academia. He is author of *Frequency Selective Surfaces, Theory and Design* (New York: Wiley, 2000). He holds numerous patents, including the Hybrid Radome Patent; and is the inventor of the four legged loaded element, and coinventor of the three-pole element (Pelton).

Dr. Munk received a Special Citation from General Loh, WPAFB in 1981 for his contributions to the U.S. Air Force, and in 1993 he received the George Sinclair Award for "Pioneering Advances in Frequency Selective Surfaces." From 1981 to 1985, he was an IEEE Antenna and Propagation Society Distinguished Lecturer. He received the Best Paper Award from the ESL in 1974, was a co-recipient of the Best Published Paper Award from Lockheed Corporation in 1982, and received the OSU College of Engineering Research Award in 1984. He is listed in *American Men and Women of Science* (12th edition).

Glenn D. Boreman (SM'98) received the B.S. degree in optics from the University of Rochester, Rochester, NY, in 1978 and the Ph.D. in optical sciences from the University of Arizona, Tucson, in 1984.

Since 1984, he has been on the faculty of the University of Central Florida in Orlando, where he is currently Trustee Chair Professor of Optics, Physics, Electrical Engineering, and Material Science. He is coauthor of *Infrared Detectors and Systems* (New York: Wiley, 1996), author of *Basic Electro-Optics for Electrical Engineers* (Bellingham, WA: SPIE, 1998) and *Modulation Transfer Function in Optical and Electro-Optical Systems* (Bellingham, WA: SPIE, 2001). His research interests include infrared and millimeter-wave sensing, and the transition of radiofrequency concepts such as antennas and frequency-selective surfaces to optical frequencies using electron-beam lithography.

Prof. Boreman is a Fellow of the Optical Society of America (OSA) and of the Society of Photo-Optical Instrumentation Engineers (SPIE). He served six years as Editor-in-Chief of OSA's journal *Applied Optics*, and is a past member of the SPIE Board of Directors. Along with his students, he received the 1995 Kingslake Medal from SPIE.